



A NEW CONCEPT FOR SOLID SURFACE DEPLOYABLE ANTENNAS

S. D. GUEST and S. PELLEGRINO

Cambridge University Engineering Department, Trumpington Street, Cambridge CB2 1PZ, U.K.

(Received 15 March 1995)

Abstract—This paper presents a new class of rigid-panel deployable antennas. The antenna surface is divided into a series of panels, which fold by wrapping around a central hub. All connections between the panels are made by revolute joints. This new folding technique has significant advantages over previous concepts, both in terms of packaged size, and mechanical simplicity. Furthermore, the size and shape of the packaged reflector can be readily adapted to any particular set of mission requirements. A small hardware demonstrator, which has been designed, manufactured and successfully tested, is discussed in the paper. Copyright © 1996 Elsevier Science Ltd

1. INTRODUCTION

Deployable antennas are an essential element of future space technology. The maximum diameter of launch vehicles limits the diameter of a satellite to about 4 m, but antennas larger than this are required for earth observation, astronomy and communications. This paper presents a new class of rigid-panel deployable reflectors where the panels fold by wrapping around a central hub, and all connections are by means of revolute joints. During deployment the panels unwrap and rotate around the hub, as shown in Fig. 1.

Deployable antennas can be split into two broad categories, those with a furlable reflector surface and those with a solid reflector surface. Furlable antennas are antennas where the surface itself can be folded; when deployed, the reflector surface is stretched out to form the required shape. Mesh antennas and inflatable antennas are both in this category.

Previously, most deployable antennas have been of the furlable type, as it is considerably easier to fold a flexible structure. The main drawback of furlable antennas is that only a limited surface accuracy can be achieved. For diameters of 10–15 m, a reasonable limit on surface accuracy appears to be 2 mm rms. A surface accuracy of 1.55 mm rms was reported for a 15 m model of the Harris Corporation Hoop Column Antenna[1], while ESA and Contraves have designed a 10 m inflatable antenna to achieve a surface accuracy of 2 mm rms[2]. Recently, attempts have been made in Japan to improve these accuracies using a Tension Truss Antenna for the VLBI Space Observatory Program[3].

Reflective surfaces are typically required to have rms accuracies in the range $\lambda/100$ – $\lambda/25$, depending on the application, where λ is the wavelength of the signal. The reported accuracies for furlable antennas

show that they are limited to frequencies below approximately 5 GHz, but there is a well established need for large antennas which can operate at higher frequencies, where solid reflectors will be required [4].

This paper considers antennas that have a solid reflective surface, but still only require a simple, autonomous deployment mechanism. Such antennas are capable of achieving accuracies an order of magnitude greater than is possible with furlable antennas and hence greatly extend the range of frequencies that can be covered by simple deployable structures. High performance reflectors that would be required for, e.g., infra-red telescopes, which require accuracies of the order of 1 μ m rms, are beyond the scope of this paper. These high accuracies can only be achieved if the reflective surface has a supporting structure, and hence either an extremely complex deployment mechanism, or some erectable components[5, 6].

The layout of the paper is as follows. Section 2 is a brief review of existing concepts for solid surface antennas with a simple autonomous deployment mechanism. Section 3 then presents the Solid Surface Deployable Antenna (SSDA), a new general concept from which many different antennas can be generated. Some of the more promising implementations of the concept are discussed. Section 4 describes in detail a particular SSDA design which was selected for an initial proof of concept demonstration, leading to the manufacture and testing of a 1.48 m diameter working model. Section 5 compares the packing efficiency of the new concept with other concepts.

2. RIGID-PANEL DEPLOYABLE ANTENNAS— STATE OF THE ART

All previously proposed rigid-panel deployable antennas consist of a central hub with radial petals,

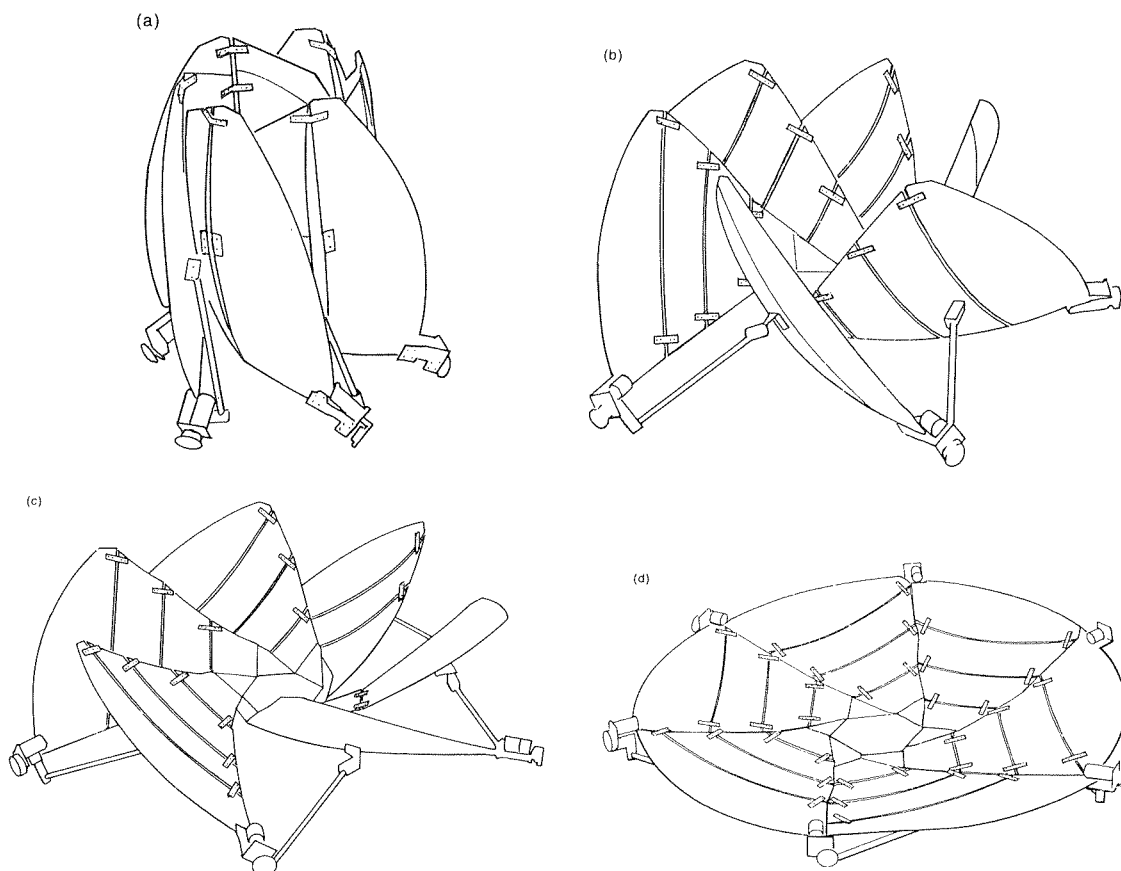


Fig. 1. Deployment sequence of the SSDA, line drawings taken from photographs of the model described in Section 4.

but they differ in the way these petals fold. This section describes the three folding concepts which have emerged and, for each concept, a number of antennas that have been built. Important characteristics of each of these antennas are compared in Table 1 with the SSDA, the new concept developed in this paper.

In the first existing concept the petals emanating from the hub fold back to back in front of the

hub. The first antenna of this type was the TRW Sunflower [7], shown in Fig. 2. It folds using only simple revolute joint connections between the panels, but does not achieve a great reduction in size. It is reported to be capable of achieving an rms surface accuracy of 0.13 mm for a 10 m diameter antenna.

Another, more complex variant on the same theme, has been developed by Toshiba/NASDA

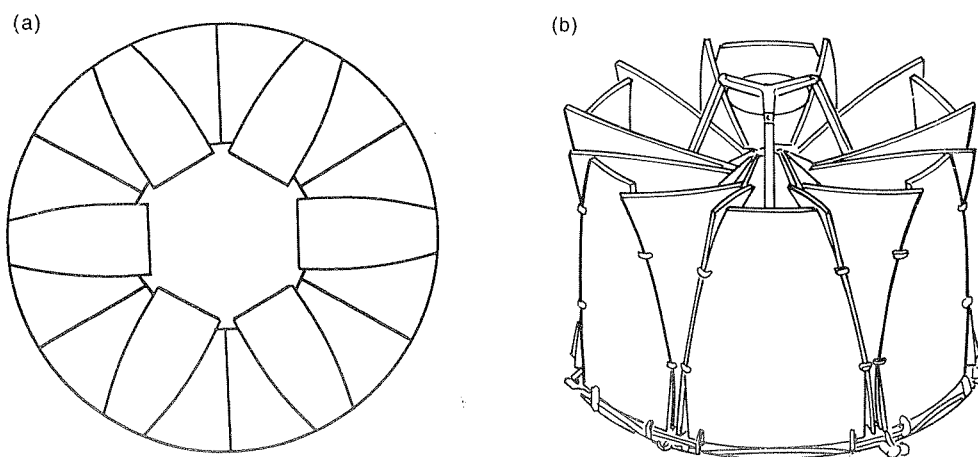


Fig. 2. TRW Sunflower: (a) deployed, plan view; (b) folded.

Table 1. Comparison of different antenna concepts

Concept	d/D	d/D	no. of panels
TRW Sunflower	0.44	0.37	19
Dornier/ESA DAISY/MEA	0.36	0.51	25
Toshiba Model 1	0.36	not known	25
Toshiba Model 2	0.36	not known	25
TRW Extended Sunflower	0.29	0.43	55
SSDA (5 panel, 6 side model)	0.37	0.54	31
SSDA (5 panel, 6 side estimate)	0.29	0.50	31
SSDA (4 panel, 6 side estimate)	0.31	0.50	25
SSDA (7 panel, 6 side estimate)	0.24	0.50	43
SSDA (7 panel, 8 side estimate)	0.34	0.38	55

in Japan [8]. It relies on more complex connections between the panels, but achieves a better packaged size. In Table 1 it is described as Toshiba Model 1.

An extended version of the Sunflower has been reported [5], and is shown in Fig. 3. It is not clear from the literature how this concept works. It appears to have lost the elegant simplicity of the original Sunflower, but can achieve a much improved packing efficiency.

In the second existing concept the petals, emanating from the central hub, are connected to it by a revolute joint, which allows the panels to fold by nesting in front of the hub. An example of this is the Dornier/ESA FIRST antenna, shown in Fig. 4. This antenna has been designed to achieve a high surface accuracy of $8\text{ }\mu\text{m}$ for an antenna of 8 m diameter and hence each panel has its own supporting truss structure[9]. Another example of this second concept has also been developed by Toshiba/NASDA [8], and is entered in Table 1 as Toshiba Model 2.

The third existing concept has a very similar final folded form to the second concept, with petals nested in front of the central hub. However, folding is achieved by a more complex joint between each petal and the hub, which allows rotation about two axes. To compensate for the increased kinematic freedom of the petals, panel-panel connecting rods are introduced, linked to the panels by spherical joints. To

fold, each panel rotates inward, and also twists, about its connection with the central hub. An antenna of this type is the Dornier/ESA MEA reflector[10]. A computer simulation of the deployment of the MEA reflector is shown in Fig. 5. The MEA reflector is designed for communications at 20–30 GHz. It has a 4.7 m diameter, and can achieve a 0.2 mm rms surface accuracy. A full-size model of this antenna has been manufactured and tested.

3. SOLID SURFACE DEPLOYABLE ANTENNA (SSDA)

This section presents the SSDA, a new concept for foldable antennas with solid reflector surfaces. The concept took its inspiration from a wrapping fold pattern for a thin flat membrane described by Guest and Pellegrino[11].

The core of the SSDA concept is shown in Fig. 6. Figure 6(a) shows an antenna surface split into *wings*; each wing is further subdivided into *panels* which are connected together by revolute joints. Figure 6(b) shows how these wings and panels fit together after folding. The panels are shown flat in the figure for clarity, but in practice the panels would of course be curved. This method of packaging a reflector surface has a number of inherent advantages:

- (i) The curved panels nest inside one another, and so they are packaged efficiently.
- (ii) The panels are connected to one another with simple joints, which are less expensive and more reliable than any alternatives.
- (iii) The concept is extendable to any number of wings and any number of panels, theoretically allowing any packaging ratios to be achieved.

Figure 6 is a considerable oversimplification of the actual kinematic design of the SSDA. Ideally, a deployable antenna should be a mechanism with a single degree of freedom, that is, only one possible way of folding or deploying. The mechanism shown in Fig. 6 obviously has many degrees of freedom, and

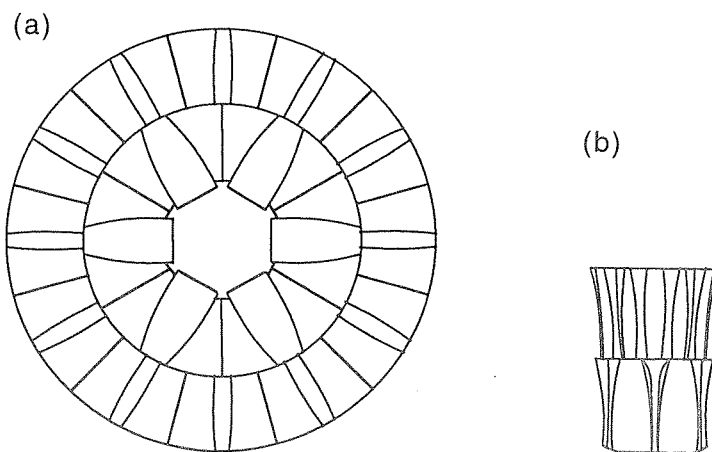


Fig. 3. TRW Extended Sunflower: (a) deployed, plan view; (b) folded, side view.

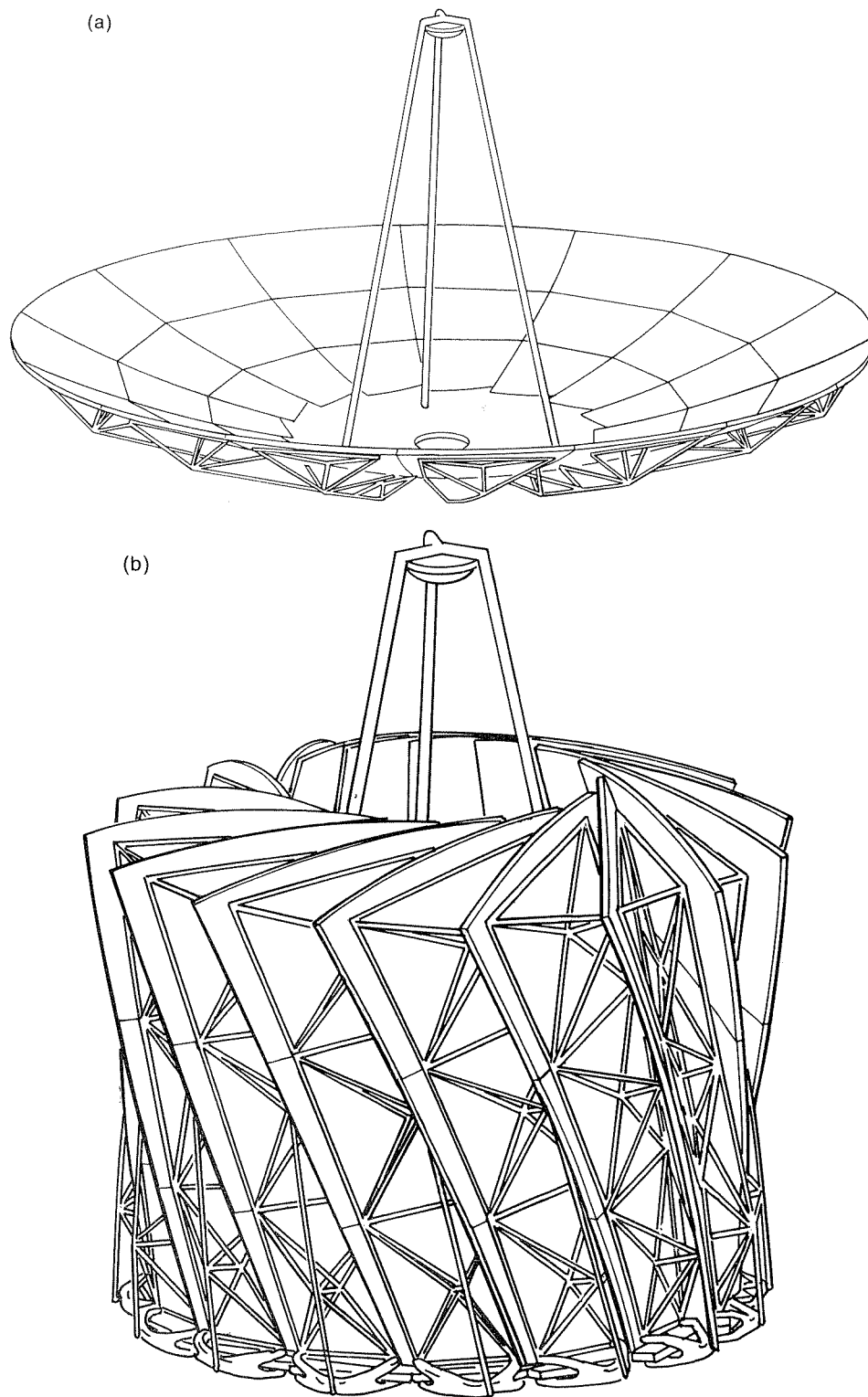


Fig. 4. Dornier/ESA DAISY antenna: (a) deployed; (b) folded.

so a suitable number of kinematic constraints must be added. These modifications are based on the idea of the *mobility* of a mechanism.

A rigid body free in space has 6 degrees of freedom. Consider n bodies in space. If one body is taken as

a reference, this leaves $6(n - 1)$ relative degrees of freedom. Now consider these bodies connected together by j joints: joint i imposes a number of constraints, u_i . For instance, a revolute joint imposes 5 constraints and a spherical joint imposes 3 con-

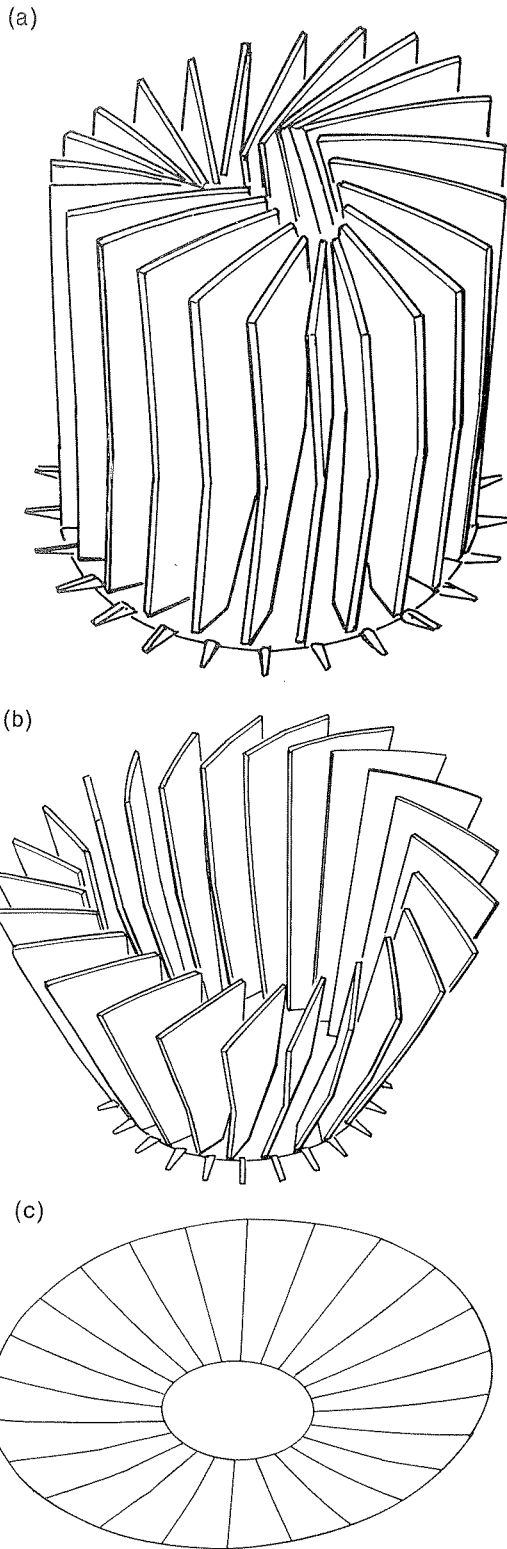


Fig. 5. Computer simulation of the deployment of the Dornier/ESA MEA reflector. Connecting bars between panels have been omitted for clarity.

straints. The number of relative degrees of freedom between the bodies when the constraints have been imposed is called the relative mobility, M , of the

system. Thus

$$M = 6(n - 1) - \sum_{i=1}^j u_i. \quad (1)$$

It should be noted that the above formula for mobility applies when the constraints are independent. Thus there will be instances when a mechanism has a greater mobility than that predicted by eqn (1). Also, eqn (1) does not imply that a mechanism with mobility greater than zero can move between all possible configurations; it may be necessary to dismantle and re-assemble the mechanism in order to reach some of these configurations. Despite these limitations, calculating the mobility of a candidate design for a deployable antenna using eqn (1) is a useful first step in selecting possible designs for the SSDA.

Consider for instance the SSDA shown in Fig. 6. This particular pattern has a hub with $s = 6$ sides, and $p = 5$ panels in each wing. There are 31 rigid bodies, 30 panels and the hub, and 30 revolute joints between the panels. Because each revolute joint imposes 5 constraints, the mobility of this system is

$$M = 6 \times (31 - 1) - 5 \times 30 = 30.$$

In general an SSDA having a hub with s sides, and p panels in each wing, will have a mobility given by

$$M = ps.$$

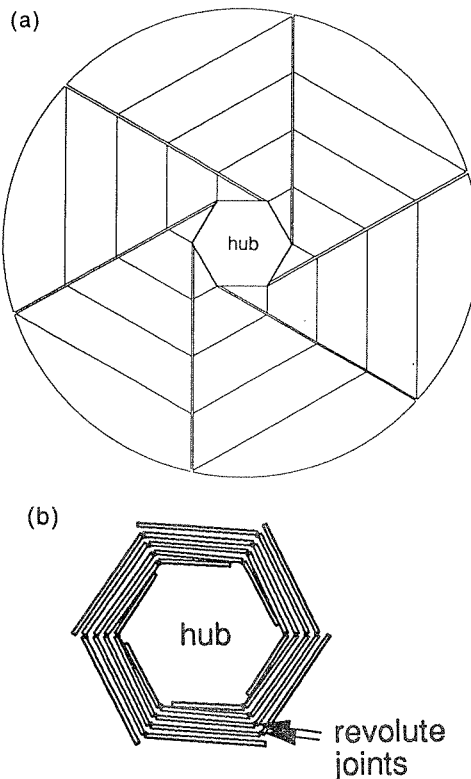


Fig. 6. SSDA: (a) Plan view of deployed surface split into wings and panels; (b) plan view of folded surface, showing wings wrapped around a central hub.

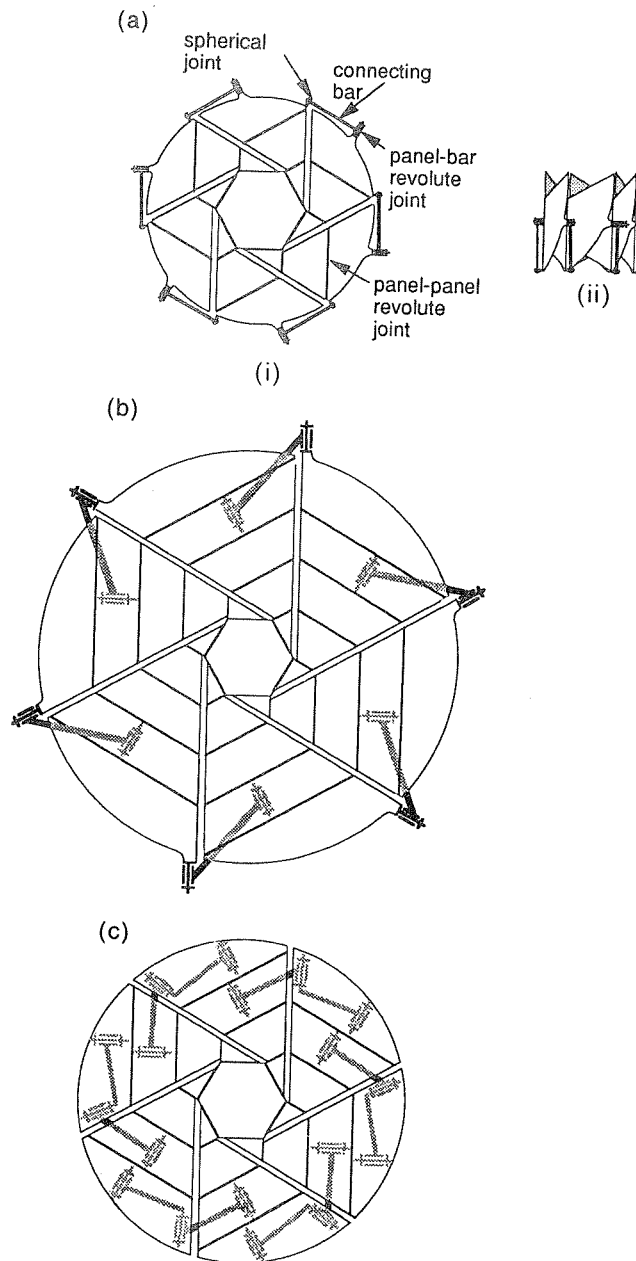


Fig. 7. Schematic views of three variants of the SSDA: (a) three panels/wing (i) deployed, (ii) folded; (b) five panels/wing; (c) four panels/wing.

Thus for any p and s the system has many degrees of freedom. There are a number of different variants of the SSDA which reduce this freedom by having a *connecting bar* between successive wings. Extra constraints can also be added by requiring that the deployment process be symmetric, for instance by coupling the motion of the panels next to the hub, or by driving each wing by a motor and running all motors at the same rate. This will add $s - 1$ constraints to the system. The ultimate aim is to have a mechanism with one degree of freedom. A

number of different ways of achieving this, at least according to eqn (1), are shown in Fig. 7, for the case $s = 6$.

Figure 7(a) shows a system where the connecting bar is linked via a revolute joint to one wing, and by a spherical joint to the adjoining wing. Each wing is made up of $p = 3$ panels, and a symmetry constraint is imposed, which leaves a system with only one degree of freedom, as shown by eqn (1)

$$M = 6 \times (25 - 1) - 5 \times 24 - 3 \times 6 - 5 = 1.$$

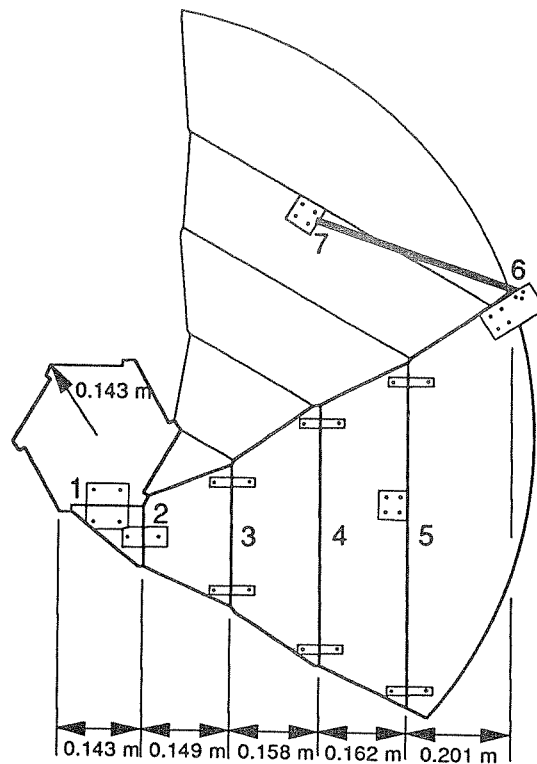


Fig. 8. Final design of the proof-of-concept SSDA.

Here 25 is the total number of bodies, including the hub, the panels and the connecting bars; 24 is the total number of revolute joints, each imposing 5 constraints; 6 is the total number of spherical joints, each imposing 3 constraints; 5 is the total number of symmetry constraints. An obvious disadvantage of the system shown in Fig. 7(a) is that it does not show a large reduction in diameter during folding.

An arrangement which produces improved packing is shown in Fig. 7(b). Here each wing is made up of 5 panels, and the connecting bars have revolute joints at both ends. For this system, eqn (1) gives

$$M = 6 \times (37 - 1) - 5 \times 42 - 5 = 1.$$

Unfortunately, eqn (1) is oversimplified, and a more careful investigation shows that this mechanism is actually overconstrained. The reason for this can be found by considering more carefully the layout of the revolute joints in a wing. In order to wrap around the central hub, the concept of the SSDA relies on all the hinges between panels being parallel. Thus, for this particular design there must be four parallel revolute joints. The overconstraint this causes can most easily be explained by considering a chain of four bodies in two dimensions; each body is connected to the next by a revolute joint and the first body is fixed to a foundation by a revolute joint. A simple analysis would conclude that the final body in this chain has 4 degrees of freedom, one for each revolute joint. However, a body in two dimensions can have at most

3 degrees of freedom. Hence, 4 parallel revolute joint provide the end body in a chain with only 3 degrees of freedom. Equation (1) does not take account of this, and so the SSDA shown in Fig. 7(b) actually has less freedom than is predicted, and is hence overconstrained.

Despite these problems, and because this scheme produces a large reduction in diameter during folding, it was this variant that was selected for further investigation. Section 4 describes a 1.5 m diameter demonstration model which has been built and tested. This model is shown unfolding in Fig. 1.

A third variant of the SSDA is shown in Fig. 7(c). In this case the connecting bar is in two separate pieces, connected by revolute joints to each other, and to adjoining wings. This particular design avoids the problem of overconstraint by only having three parallel hinges in each wing, but has a lower packing efficiency than the previous variant. However, it is possible to extend this particular packaging scheme by adding more panels in each wing. For example, to improve the packing efficiency of the SSDA shown in Fig. 7(c), another three panels could be added to each wing, with another two-piece connecting bar at the end. Further extensions of such a system would be possible using virtually the same design. The problem of having more than three parallel hinges will not occur in these extended examples, as there are never more than three parallel hinges within a single loop of the mechanism.

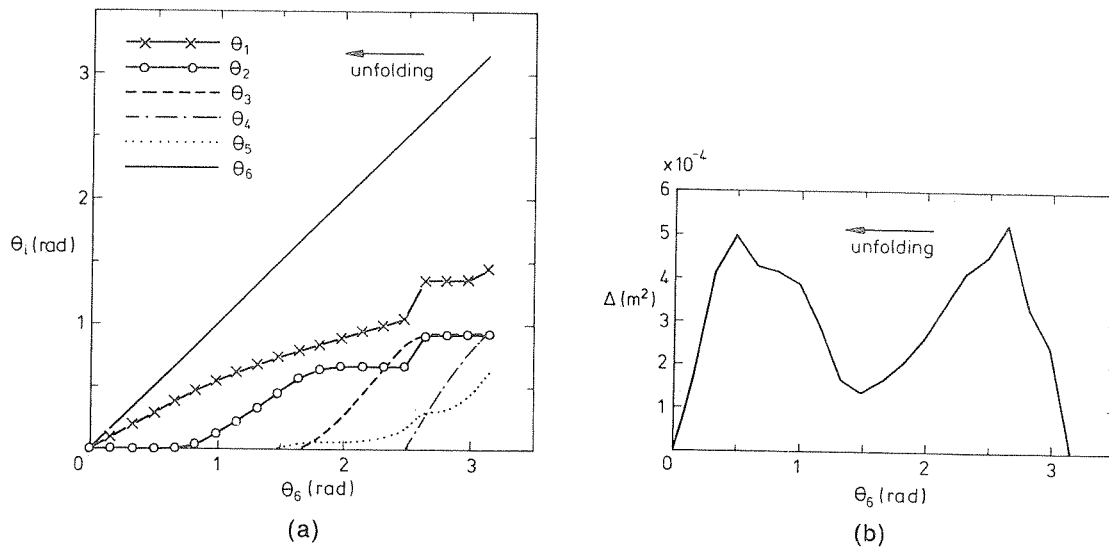


Fig. 9. Deployment of SSDA: (a) angles turned by each hinge during deployment; (b) deformation required during deployment.

4. A PROOF-OF-CONCEPT MODEL

An SSDA with a six-sided hub, five panels per wing and a connecting bar having revolute joints at both ends was selected for further study. A model of this antenna was designed and made. This model was meant to prove the viability of the concept of the SSDA, and not to be a development prototype for

space hardware. There are aspects which would not be acceptable in a real antenna, but it is expected that only minor design changes would be required to produce a better prototype.

4.1 Design

The design process consisted of two parts. In the first part, the shape of the panels was calculated by

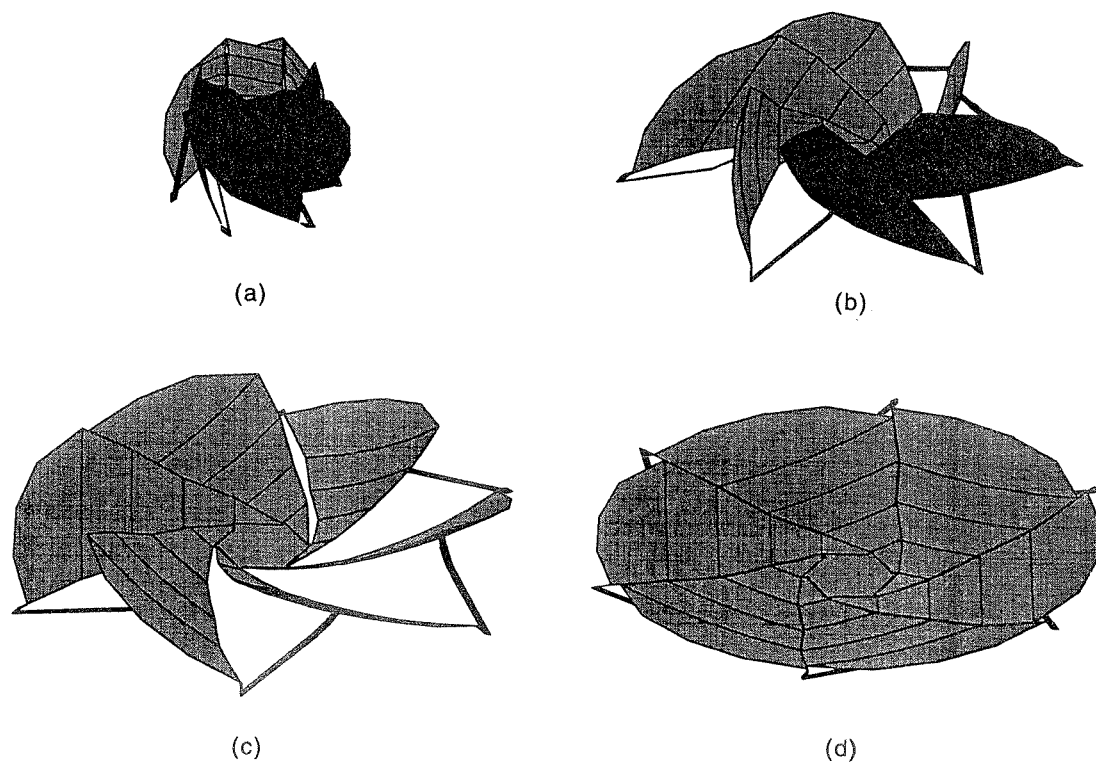


Fig. 10. Four views from a computer simulation of the deployment of the optimized SSDA, for (a) $\theta_6 = 3.34$ rad; (b) $\theta_6 = 2.23$ rad; (c) $\theta_6 = 1.11$ rad; (d) $\theta_6 = 0$ rad.

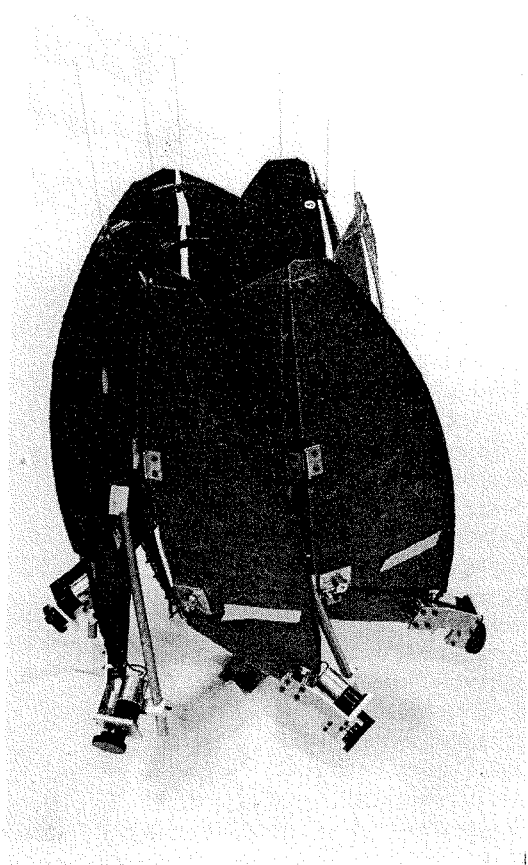


Fig. 11. SSDA proof of concept model, fully folded.

considering the constraints imposed by the concept of the SSDA, i.e. that the hinges between panels must be parallel, and that they must wrap around the hub in the way shown in Fig. 6(b). In the final design the panels were not designed to wrap around the hub as evenly as shown in Fig. 6(b). The spacing between hinges which wrap next to one another was varied. The radial distance between adjacent hinges in the folded configuration was 13 mm between the first and second hinge, 5 mm between the second and third hinge, 2 mm between the third and fourth hinge and 62 mm between the fourth hinge and the edge of the panel. A minimum value for the spacing was obtained by considering the packaged shape of the antenna, but some values were increased to prevent collisions between panels during unfolding. These particular values were chosen in the light of results from a series of unfolding simulations, described below. The larger gap between the final hinge line and the edge of the last panel was required to leave room for the connecting bar. The spacing between some hinges may seem rather small, and in one case is actually less than the thickness of the antenna surface used, but as the panels are curved, and so nest inside one another, they are actually fairly conservative.

By using the values given above, and ensuring that the outside of the antenna coincides with the edge of the last panel, the radius of the hub in the final design

was fixed at 0.143 m. Thus the panels have widths of 0.143 m, 0.149 m, 0.158 m, 0.162 m, and 0.201 m. This design is shown in Fig. 8. Note that the shape of the panels is a little more complex than in the earlier schematic diagrams. This is because the parallel hinge lines are now laid out to intersect the parabolic surface at points where the actual connections between panels are made.

In the second part of the design process the position of the connecting bar and the orientation of the revolute joints at its ends were varied in order to optimise the deployment behaviour of the model. First, several attempts were made at finding a design that allows strain-free folding. However, these attempts were unsuccessful because any SSDA based on the scheme of Fig. 7(b) is an overconstrained mechanism, as was explained in Section 3. After these problems were identified, the design aim shifted to finding a position of the connecting bar which minimised the deformation of the surface during unfolding.

This problem was simplified by modelling the antenna panels as rigid bodies, and assuming that all of the deformation is concentrated at six hinges only, one at the end of each connecting bar. For each trial design, the unfolding of the SSDA was simulated to obtain an estimate for the maximum deformation required to go from the fully folded to the fully deployed configuration. An optimal position of the connecting bar and orientation of its hinges were thus obtained. The simulation technique and the optimisation process are described in full elsewhere [12, 13]. The results for the optimal design are shown in Fig. 9. Figure 9(a) shows the angles turned by hinges 1–6, defined in Fig. 8, as hinge 6 is turned. The hinge rotations are defined with reference to the fully deployed configuration, where every angle equals zero. Initially, in the fully-folded configuration, $\theta_1 = 1.43$ rad, $\theta_2 = 0.91$ rad, $\theta_3 = 0.93$ rad, $\theta_4 = 0.96$ rad, $\theta_5 = 0.62$ rad, $\theta_6 = 3.34$ rad. As θ_6 is gradually decreased, hinges 3, 4, and 5 turn faster than the others and are the first to reach their stops. Hinge 2 then speeds up and reaches its stop. In the final stage of deployment, only hinges 1 and 6 are still turning. Figure 9(b) plots the deformation, Δ , of the antenna during deployment, where Δ is defined as the sum of the squares of the misfits at two points lying 100 mm apart on the line of hinge 7. The maximum misalignment at these points is predicted to be 15 mm for a 1.5 m antenna, which in reality will be distributed over all of the panels in the model, and hence will only require a small amount of deformation. Four views of the antenna, taken from this numerical simulation, are shown in Fig 10.

4.2 Manufacture

The model has a radius of 0.74 m and a focal length/diameter ratio of 0.42, so the outer edge of the antenna is 0.22 m above its centre. The surface is made from 3 mm thick glass-fibre, moulded over an existing axisymmetric parabolic Al-alloy antenna.

Simple brass hinges were used as revolute joints. They were accurately bolted to the uncut surface, using carefully machined spacers to ensure that the two hinges on one revolute joint were correctly aligned. Hinge stops were bolted to the rear of the panels at each hinge line to prevent the joint from rotating past its deployed configuration. The surface was then cut into panels.

The connecting bar is an Al-alloy tube with an outside diameter of 16 mm, and a wall thickness of 0.5 mm. It connects panel 5 on one wing to panel 4 on the next. The joint between the connecting bar and panel 5 is driven by a heavily geared down DC electric motor. The whole joint assembly is accurately bolted to panel 5. The joint at the other end of the connecting bar is a simple brass hinge, similar to those connecting the panels. This hinge is connected to panel 4 by an Al-alloy bracket, which was carefully manufactured to ensure that the axis of the hinge is correctly positioned.

A simple gravity compensation system supports each wing of the model. A wire is attached to the outer panel, close to the motorised hinge assembly, as this represents a significant part of the weight each wing has to carry. The wire runs over a pulley to a counter-weight. The pulley itself is mounted at the tip of a bar which can rotate about a vertical hinge, and this arrangement allows the wire to remain vertical during deployment.

4.3 Performance

The model deploys successfully by simultaneously running all 6 motors. Typically, a complete deployment takes 30 s. Figure 1 shows four line drawings of the model, taken from photographs of the reflector during deployment. These views are very similar to the corresponding views produced by the numerical simulation, shown in Fig. 10. A photograph of the model when fully folded is shown in Fig. 11.

During deployment of the model there is some evidence of the two deformation peaks predicted by the simulation, and shown in Fig. 9. When $\theta_6 = 2.70$ rad the simulation predicts that the antenna will reach the first deformation maximum. At this point the simulation predicts that hinge 1 will suddenly start turning, and this is observed in practice, as the hinges connected to the hub quickly start to open. Also, the simulation predicts a second peak in deformation when $\theta_6 = 0.54$ rad, and in practice at this point the antenna suddenly snaps through to the final, deployed configuration.

The model successfully deploys without any manual intervention, but it requires some help to fold back correctly. The problem is that when the 6 motors are turned in the opposite direction, to fold the fully-deployed model, the model attempts to take an incorrect path when $\theta_6 \approx 2.7$ rad, i.e. where Fig 9(b) shows the first deformation peak during deployment. However, the model can be easily guided manually towards the correct path at this point, and

then completes folding without further intervention. This problem is due to the deformation that the antenna has to undergo during deployment, and would not occur on other variants of the SSDA which have a strain-free deployment.

5. DISCUSSION

The model antenna is 1.48 m in diameter. When folded, it fits into a cylindrical envelope, 0.55 m in diameter and 0.80 m long. Defining the initial antenna diameter as D , and the final package dimensions as diameter d and length l , this gives a d/D ratio of 0.37, and an l/D ratio of 0.54. A new version of the current design, with only simple changes, could considerably reduce these ratios. With a more careful design of the connecting bar and less conservative gaps between panels, the reflector could fit into a cylindrical envelope 0.43 m in diameter and 0.74 m long. This would reduce the packaging ratios to $d/D = 0.29$ and $l/D = 0.50$.

Table 1 compares the SSDA with other published concepts of deployable antennas based on solid panels. The comparison includes the packaged diameter and length of each antenna as well as the number of panels used, which is a crude measure of complexity. As well as including the packaging ratios achieved by the SSDA proof of concept model, the table gives the ratios that could be obtained from a new version of the SSDA, as discussed above. The table also estimates the packaging ratios of three other variants of the SSDA.

The most critical dimension of a payload is generally its diameter, and hence the parameter d/D is the most important packaging ratio. By this measure the SSDA, even in its present primitive form, packs as well as the DAISY/MEA and both Toshiba concepts, and considerably better than the TRW Sunflower. With the simple improvements outlined above, a reflector similar to the current model will have a d/D ratio equal to that of the TRW Extended Sunflower, and considerably better than any other concept. Note that, however, the Extended Sunflower requires a very large number of panels.

Comparing packaged lengths of the reflectors, the proof of concept SSDA does not pack as well as either TRW Sunflower. However, the other concepts fold entirely in front of the hub, and so all of the space within their packaged envelopes is fully used, while the SSDA wraps around the hub, leaving space both in front of, and at the rear of the hub that could be used for other equipment, e.g. the antenna pointing mechanism.

The estimates for other SSDA variants show the versatility of the SSDA concept, allowing considerable improvements in packaged diameter with only a moderate increase in complexity.

The packaged length of the SSDA can be made as low as required by changing the number of sides of the hub. Table 1 shows that a significant improve-

ment in packaged length can be obtained by using an 8-sided rather than a 6-sided hub.

In conclusion, this paper has described a new type of deployable reflector, the SSDA. The design philosophy behind this antenna is to keep all of the mechanical components as simple as possible. Thus, although the geometry and the overall design process are more complex than in other concepts, the hardware is quite simple. Furthermore, the SSDA concept is very flexible, and can achieve any required packaging ratios. To develop the SSDA into a flight-ready mechanical design would not require new technology; the level of technology would certainly be simpler than that required by, e.g., the MEA reflector.

Acknowledgements—We would like to thank J. F. Clemmet and R. Dace of Matra Marconi Space Systems for their help and encouragement with this work. Financial support from EPSRC and Matra Marconi Space Systems is gratefully acknowledged.

REFERENCES

1. G. Campbell, M. C. Bailey and W. K. Belvin, The development of the 15-meter Hoop Column Antenna System with final structural and electromagnetic results. *Acta Astronautica* **17**, 69–77 (1988).
2. W. V. T. Rusch, The current state of the reflector art—entering the 1990's. *Proceedings of the IEEE* **80**, 113–126 (1992).
3. K. Miura and Y. Miyazaki, Concept of the tension truss antenna. *AIAA Journal* **28**, 1098–1104 (1989).
4. C. A. Rogers, W. I. Stutzman, T. G. Campbell and J. M. Hedgepeth, Technology assessment and development of large deployable antennas. *ASCE Journal of Aerospace Engineering* **6**, 34–54 (1993).
5. J. M. Hedgepeth, Structures for remotely deployable precision antennas. NASA CR-182065 (1989).
6. H. G. Bush, C. L. Herstrom, W. L. Heard Jr., T. J. Collins, W. B. Fichter, R. E. Wallson and J. E. Phelps, Design and fabrication of an erectable truss for precision segmented reflector application. *Journal of Spacecraft and Rockets* **28**, 251–257 (1991).
7. J. S. Archer and W. B. Palmer, Antenna technology for QUASAT application. *Large Satellite Antennas and Space Technology*. NASA CR-2368 part 1 (1984).
8. Y. Tsutsumi, A. Kasahara, Y. Hisadi and Y. Itoh, Study on solid surface, deployable antenna reflector. Proceedings, 2nd Workshop on Mechanical Technology for Antennas. ESA SP-261, 41–45 (1986).
9. Dornier, FIRST Technology study: multisurface control mechanism for a deployable antenna. Final report. Dornier Report RP-FA-D003 (1987).
10. P. Specht, Dynamics of large reflectors: DAISY/MEA reflector—description. Dornier Technical Report 2100-2 (1990).
11. S. D. Guest and S. Pellegrino, Inextensional wrapping of flat membranes. *Proceedings, First International Seminar on Structural Morphology*, Montpellier, La Grand Motte, 7–11 September 1992 (Edited by R. Motro and T. Wester), LMGC, Universite Montpellier II, 203–215 (1992).
12. S. D. Guest, Deployable structures: concepts and analysis. PhD dissertation, University of Cambridge (1994).
13. S. D. Guest and S. Pellegrino, Design optimisation of a solid surface deployable reflector. *Proceedings, IUTAM Symposium on Optimisation of Mechanical Systems*, Stuttgart, 26–31 March 1995 (Edited by D. Bestle and W. Schielen), 105–112, Kluwer, Dordrecht (1996).